Int. J. Heat Mass Transfer. Vol. 13, pp. 287–304. Pergamon Press 1970. Printed in Great Britain

LOCAL HEAT SINK ON A CONVECTIVELY COOLED SURFACE—APPLICATION TO TEMPERATURE MEASUREMENT ERROR

D. K. HENNECKE and E. M. SPARROW

Department of Mechanical Engineering, University of Minnesota, Minneapolis, Minnesota 55455, U.S.A.

(*Received* 17 *February* 1969 *and in revised form* 2 *June* 1969)

Abstract—An analysis is made of the thermal processes associated with the presence of a local heat sink (or source) on the convectively cooled surface of a solid. The sink is due to the presence of a surface-mounted thermocouple, a pin fin or other surface-mounted conductors. In the first part of the paper, heat transfer results and temperature distributions for the solid are determined in general, without reference to specific applications. The results are then applied to the case of the surface-mounted thermocouple, and the error in the measured temperature owing to the presence of the thermocouple is evaluated. Application is also made to pin fins and other surface-mounted conductors, and heat transfer rates are calculated taking into account the depression of the base temperature owing to the interaction of the fin (or conductor) and the solid. It is found that the conventional calculation which neglects the base temperature depression overestimates the heat transfer rates.

NOMENCLATURE

A, heat transfer areas of finite volume element;

$a, \ldots, e$, coefficients in equation (12);

Bi, Biot number, hr_0/k;

F, inhomogeneous factor in equation (12);

h, heat transfer coefficient;

k, thermal conductivity of solid;

$\overline{kA}$, conductivity-area product for cylindrical conductor, see equation (21);

L, length of cylindrical conductor;

Q, heat transfer rate from pin fin or cylindrical conductor;

$\tilde{Q}$, heat transfer rate from fin or conductor neglecting base temperature depression;

Q_j, rate of heat transfer passing through surface area $0 \leqslant r \leqslant r_0$, equation (16);

Q_j^*, dimensionless heat transfer rate associated with the disturbance temperature field, equation (16);

q, local surface heat flux;

R, thermal resistance, equation (21);

r, radial coordinate;

r_0, radius of circular contact region;

T, temperature;

$\tilde{T}$, undisturbed temperature distribution, equation (1);

T_j, temperature of surface area $0 \leqslant r \leqslant r_0$;

T_w, undisturbed surface temperature;

T_∞, ambient temperature;

x, axial coordinate along thermocouple;

Z, dimensionless axial coordinate in solid, z/r_0;

z, axial coordinate in solid.

Greek symbols

ϑ, θ, dimensionless disturbance temperature, equation (2);

ρ, dimensionless radial coordinate, r/r_0;

φ, ϕ, angular coordinate;

χ, conductance ratio, equation (24).

Subscripts

f, fin;
i, j, value at nodal point i, j;
surf, value at surface.

INTRODUCTION

THIS paper is concerned with the heat transfer processes and attendant temperature field associated with the presence of a cylindrical heat conductor affixed to the convectively cooled surface of a solid. The conductor itself may exchange heat with the fluid environment, either directly or through a layer of insulation. Such a physical situation is illustrated schematically in Fig. 1(a). The cylindrical conductor may be either straight or curved*, either insulated or uninsulated.

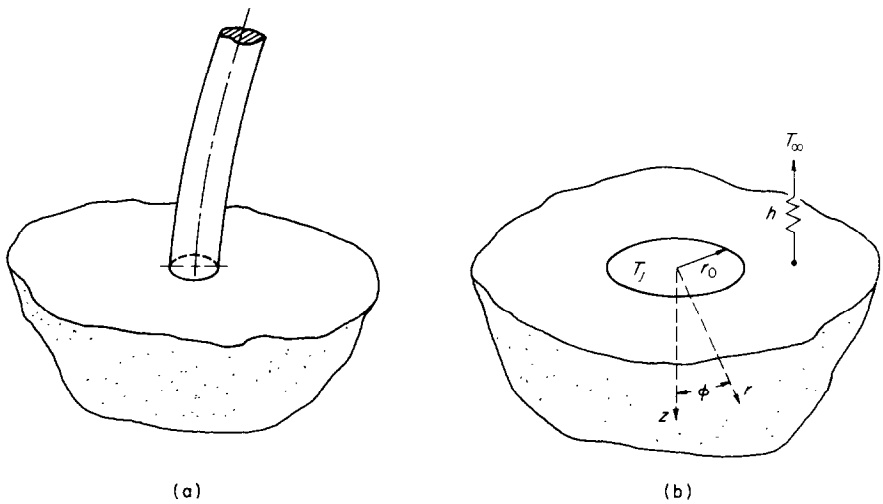

FIG. 1. Schematic representation of the physical situation.

Consideration of the aforementioned problem is motivated by, among other applications, the measurement of surface temperature of solids. The measurement may be performed by a thermocouple affixed to the surface. Although by no means optimal from the standpoint of measurement accuracy, thermocouple installations that are more or less similar to that of Fig. 1(a) are quite common in practice. Typically, a thermocouple installed in this way conducts heat away from the surface at a greater rate than that associated with the convective exchange between the surface and the fluid environment. As a consequence, the presence of the thermocouple causes a local depression of the temperature of the solid, with the result that the thermocouple output is not indicative of the surface temperature of the undisturbed solid.

In addition to the determination of errors in surface temperature measurement, the results of the present analysis are applicable to the heat transfer and temperature fields associated with surface-mounted cylindrical heat conductors in general. In particular, the heat transfer from pin fins can be evaluated, taking account of the depression of the fin base temperature owing to the presence of the fin.

The analysis presented herein is carried out for steady-state operating conditions. In formulating the problem, it is assumed that the dimensions of the solid are large compared with the radius of the circle of contact of the surface

* The radius of curvature must be large compared with the radius of the conductor.

with the conductor. In reality, as demonstrated by the results, the solid need not be very large to fall within the framework of the analysis. In the formulation, it is also assumed that the conductor has sufficiently high thermal conductivity and/or sufficiently small cross section so that the temperature of the surface within the circle of contact is spatially uniform.

There appears to be very little in the published literature that bears directly on the subject matter of the present investigation. An analysis of the transient response of a surface-mounted thermocouple affixed to a semi-infinite body is reported in [1], the analytical model being spatially one-dimensional and, therefore, not closely related to the present two-dimensional formulation and solution. The steady-state heat flow through a circular isothermal zone on the otherwise insulated surface of a semi-infinite solid is determined by an elegant analysis in [2]. The insulated surface condition is a special case of the convective boundary condition treated herein, so that a limited comparison of results can be made.

A variety of physical situations, other than that investigated here, have been treated in the literature on thermocouple-related heat conduction. A sampling of such literature is discussed below. The case of a thermocouple affixed to a thin, convectively cooled plate was investigated in [3–5] with a view to assessing the conduction-induced measurement error under steady-state conditions.* A similar study is reported in [6] for a radiation-cooled plate. [7, 8] deal with thermocouple installations in transient problems characterized by prescribed surface heat flux, respectively for a surface-mounted thermocouple and an imbedded thermocouple.

In the formulation that follows, the heat transfer processes in the solid and in the conductor are, at first, decoupled. The decoupling is achieved by assigning a temperature T_j ($j \sim$ junction) to the surface of the solid that lies within the circle of contact. Although actually unknown, the junction temperature T_j can, from the standpoint of the heat transfer processes in the solid, be provisionally regarded as known. Solutions for the solid are then carried out and relevant results reported. With this information, the thermal interaction between the solid and the conductor is analyzed. Results are evaluated and presented for the difference between the junction temperature and the temperature of the surface in the absence of the conductor. In the case of a surface mounted thermocouple, the aforementioned temperature difference is the measurement error owing to the presence of the thermocouple. Heat transfer results for pin fins and for general cylindrical conductors, including the effects of surface temperature depression, are also presented.

* It was verified that for those aspects for which comparisons are possible, the results of the references are in qualitative accord with those found here.

LOCAL HEAT SINK ON A CONVECTIVELY COOLED SURFACE

In accordance with the just-discussed decoupling, consideration is now given to the heat transfer processes in the system pictured in Fig. 1(b). On the surface of the solid, the temperature within a circle of radius r_0 is prescribed to be uniform and equal to T_j. Outside this circle, the surface exchanges heat by convection with a fluid having heat transfer coefficient h and temperature T_∞.

Let T_w be the spatially uniform surface temperature in the *absence* of the local heat sink, that is, for the case in which $r_0 = 0$. When the heat sink is in place, the temperature field in the solid will, at large values of the coordinate r, asymptotically approach that which exists in the absence of the sink. Therefore, for the case in which heat sink is in place, the specification of T_w serves to specify the behavior of the temperature field at large r.

Spherical coordinates are employed herein in the formulation and solution of the problem, with r representing the radial distance and φ the cone angle. Owing to symmetry, there is no dependence on the azimuthal angle. The z

coordinate, normal to the plane of the surface, is also shown in the figure.

In formulating the problem, it is advantageous to work with a temperature variable which is the difference between the temperature fields corresponding to the presence and to the absence of the local surface heat sink. In physical terms, such a variable represents the temperature field of the disturbance caused by the presence of the sink. Furthermore, as will be demonstrated shortly, the dimensionless disturbance temperature field is independent of all of the given temperatures T_∞, T_w and T_j, an outcome which is highly favorable from the standpoint of practical computation.

To begin, it may be recognized that in the absence of the surface heat sink, the temperature field $\tilde{T}(z)$ is given by

$$\tilde{T}(z) = \frac{hz}{k}(T_w - T_\infty) + T_w. \tag{1}$$

Next, the temperature field $T(r, \varphi)$ corresponding to the presence of the heat sink is reduced by $\tilde{T}$ and made dimensionless relative to $(T_j - T_w)$, that is

$$\vartheta(r, \varphi) = \frac{T - \tilde{T}}{T_j - T_w} = \frac{T - [(hz/k)(T_w - T_\infty) + T_w]}{T_j - T_w}. \tag{2}$$

The temperature distribution $T(r, \varphi)$ must satisfy Laplace's equation, and it is readily demonstrated that the disturbance distribution $\vartheta(r, \varphi)$ must also satisfy this same equation, so that in spherical coordinates (with $\rho = r/r_0$)

$$\frac{\partial}{\partial \rho}\left(\rho^2 \frac{\partial \vartheta}{\partial \rho}\right) + \frac{1}{\sin \varphi}\frac{\partial}{\partial \varphi}\left(\sin \varphi \frac{\partial \vartheta}{\partial \varphi}\right) = 0. \tag{3}$$

Within the circular region $0 \leqslant r \leqslant r_0$ on the surface, where $T = T_j$ and $\tilde{T} = T_w$, the ϑ variable is unity. Furthermore, the convective condition $-k(\partial T/\partial z) = h(T_\infty - T)$, which applies at surface locations $r > r_0$, transforms to $\partial\vartheta/\partial z = (h/k)\vartheta$. Also, at large r, $\vartheta \to 0$. The formal statement of the boundary conditions is

$$\vartheta = 1 \quad \text{for } 0 \leqslant \rho \leqslant 1 \text{ and } \varphi = \pi/2\,(Z = 0) \tag{4a}$$

$$\partial\vartheta/\partial Z = Bi\vartheta \quad \text{for } \rho > 1 \text{ and } \varphi = \pi/2\,(Z = 0) \tag{4b}$$

$$\vartheta \to 0 \quad \text{as } \rho \to \infty \text{ for all } \varphi \tag{4c}$$

where

$$\rho = r/r_0, \quad Z = z/r_0, \quad Bi = hr_0/k. \tag{5}$$

Inspection of equations (3) and (4) indicates that the dimensionless temperature distribution ϑ depends only on a single parameter, the Biot number $Bi = hr_0/k$. It appears that amongst all finite Biot numbers, only the case of $Bi = 0$ (insulated surface) admits an analytical solution [2]. However, in employing this solution to determine ϑ at any point (r, φ) in the solid, it is necessary to numerically evaluate an integral over the range of a dummy variable from zero to infinity; furthermore, the integration must be repeated at every point at which the temperature is desired. Fortunately, the solution yields a simple expression for the overall heat flux crossing the circular region $0 \leqslant r \leqslant r_0$, $z = 0$.

For finite values of the Biot number other than zero, it is necessary to solve equations (3) and (4) by numerical means. A finite-difference approach, incorporating variable mesh spacing and making use of the method of extrapolated iterations, was employed to obtain the solutions. On the basis of preliminary computational experiments, it was found that very rapid changes in ϑ occur in the vicinity of $r = r_0$ and $\varphi = \pi/2$. To insure high accuracy in this region as well as to generally permit the local concentration of mesh points to be varied according to the local characteristics of the temperature field, the finite-difference form of the energy equation was written with variable step sizes in both r and φ.

Since finite-difference formulations in spherical coordinate systems are not commonly encountered in the literature, the derivation of the appropriate difference equations will now be outlined. In the derivation, the relevant heat transfer areas (i.e. normal to the directions of heat flow) are expressed without approximation. As will be discussed later, other discretization procedures yield only approximate representations of the heat transfer areas.

The trace in any meridional plane of the grid structure at a typical interior point* is shown in Fig. 2(a). The shaded element, which appears

$$A_{ab} = 2\pi(\rho_0 - \tfrac{1}{2}\Delta\rho')^2 \left[\cos(\varphi_0 - \tfrac{1}{2}\Delta\varphi') - \cos(\varphi_0 + \tfrac{1}{2}\Delta\varphi'')\right] \quad (6)$$

and similarly for A_{cd} with $\rho_0 - \frac{1}{2}\Delta\rho'$ replaced by $\rho_0 + \frac{1}{2}\Delta\rho''$. Furthermore, the exact representation of the area for heat flow normal to the surface *ad* (i.e. flow in the tangential direction) is

$$A_{ad} = \pi \frac{\Delta\rho' + \Delta\rho''}{2} [2\rho_0 + \tfrac{1}{2}(\Delta\rho'' - \Delta\rho')] \times \sin(\varphi_0 - \tfrac{1}{2}\Delta\varphi') \quad (7)$$

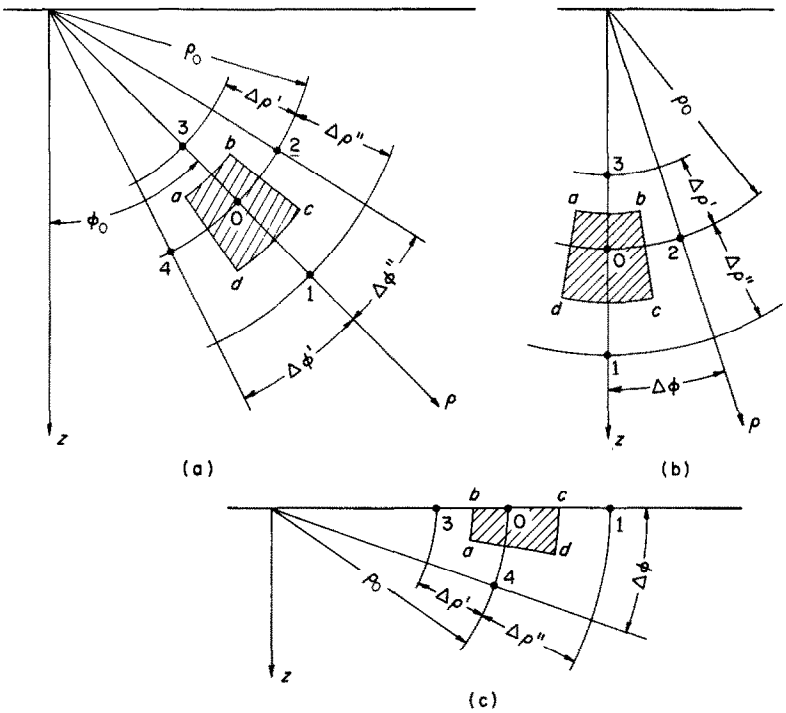

FIG. 2. Configuration and nomenclature for typical nodal points.

plane in the figure, is actually toroidal, spanning the entire 2π degrees of the azimuthal angle. The area for heat flow normal to the surface *ab* (i.e. flow in the radial direction) is expressed without approximation as

with an identical expression being applicable for A_{bc} provided that $\varphi_0 - \frac{1}{2}\Delta\varphi'$ is replaced by $\varphi_0 + \frac{1}{2}\Delta\varphi''$.

Then, in terms of the aforementioned areas and of distances shown in Fig. 2(a) and using central differences for the participating temperature derivatives, the finite-difference form

* Except points on the line $\varphi = 0$.

of the energy equation at point 0 may be written as

$$\vartheta_0 = \frac{\vartheta_1(A_{cd}/\Delta\rho'') + \vartheta_2(A_{bc}/\rho_0\Delta\varphi'') + \vartheta_3(A_{ab}/\Delta\rho') + \vartheta_4(A_{ad}/\rho_0\Delta\varphi')}{(A_{cd}/\Delta\rho'') + (A_{bc}/\rho_0\Delta\varphi'') + (A_{ab}/\Delta\rho') + (A_{ad}/\rho_0\Delta\varphi')}. \tag{8}$$

A special difference equation applies for interior points situated on the line $\varphi = 0$, which is a line of symmetry. The trace of the typical grid pattern relevant to such points is shown in Fig. 2(b). The volume element actually surrounding point 0 is that obtained by revolving the shaded element *abcd* about the symmetry axis. The lines *ad* and *bc* lie on a conical surface whose area is

$$A_{\text{con}} = \pi \frac{\Delta\rho' + \Delta\rho''}{2} [2\rho_0 + \tfrac{1}{2}(\Delta\rho'' - \Delta\rho')] \sin\frac{\Delta\varphi}{2}. \tag{9}$$

The expressions for A_{ab} and A_{cd} have a form similar to that of equation (6), but now the quantity in brackets is replaced by $[1 - \cos(\Delta\varphi/2)]$. By employing these areas and central differences for the derivatives, the energy balance for the element surrounding point 0 is

$$\vartheta_0 = \frac{\vartheta_1(A_{cd}/\Delta\rho'') + \vartheta_2(A_{\text{con}}/\rho_0\Delta\varphi) + \vartheta_3(A_{ab}/\Delta\rho')}{(A_{cd}/\Delta\rho'') + (A_{\text{con}}/\rho_0\Delta\varphi) + (A_{ab}/\Delta\rho')}. \tag{10}$$

Attention will now be turned to points on the surface of the solid which exchange heat by convection with the environment and where the boundary condition (4b) applies. The corresponding finite-difference grid is illustrated in Fig. 2(c). The area A_{ab} is given by equation (6) when the quantity in brackets is replaced by $\sin(\Delta\varphi/2)$; a similar modification is made to adapt the corresponding expression for A_{cd}. Equation (7) for A_{ad} continues to apply with $\varphi_0 = \pi/2$, and this same equation with the sine factor replaced by unity gives A_{bc}. With this information and with the boundary condition (4b), the finite-difference equation for point 0 is

$$\vartheta_0 = \frac{\vartheta_1(A_{cd}/\Delta\rho'') + \vartheta_3(A_{ab}/\Delta\rho') + \vartheta_4(A_{ad}/\rho_0\Delta\varphi)}{(A_{cd}/\Delta\rho'') + (A_{ab}/\Delta\rho') + (A_{ad}/\rho_0\Delta\varphi) + A_{bc}Bi}. \tag{11}$$

Equations that are similar, but not identical, to (8), (10) and (11) can be derived by starting with the differential equation (3) and representing the derivatives appearing therein by central differences. However, the difference equations derived by such a procedure contain approximations that are not made in equations (8), (9) and (11). These approximations arise from the fact that when the differencing procedure is applied, the differential heat transfer areas contained in equation (3) do not lead to exact representations for finite heat transfer areas. Therefore, the equations derived in the preceding paragraphs are more faithful to the finite-difference model than are those obtained from the discretization of the differential equation (3).

The participating difference equations were solved by the method of extrapolated iterations,* which will now be briefly outlined. Suppose that the mesh points are arranged in columns and rows, respectively indexed by i and j. The prototype difference equation, applicable at any point i, j, is

$$\vartheta_{i,j} = a_{i,j}\vartheta_{i+1,j} + b_{i,j}\vartheta_{i-1,j} + c_{i,j}\vartheta_{i,j+1} + d_{i,j}\vartheta_{i,j-1} + e_{i,j}F_{i,j} \tag{12}$$

where the coefficients $a, \ldots, d$ are readily identified by comparison with equations (8), (10) and (11). For mesh points characterized by

* This procedure is sometimes called the method of successive overrelaxations in the literature on numerical analysis. However, the word overrelaxation has another meaning in the heat transfer literature. To avoid confusion, no further mention will be made here of overrelaxation.

$0 \leqslant \rho \leqslant 1$ and $\varphi = \pi/2 - \Delta\varphi$, $e_{i,j}F_{i,j}$ is an inhomogeneous term related to the boundary condition (4a). At all other mesh points $e_{i,j}F_{i,j} = 0$.

Envision the grid being swept in a regular pattern, say, in the same direction along successive rows. After N sweeps, the temperatures ϑ^N at all points are known. Suppose that the $(N+1)$th sweep is in progress and that $\vartheta_{i,j}^{N+1}$ is about to be calculated, the temperatures $\vartheta_{i-1,j}^{N+1}$ $\vartheta_{i-2,j}^{N+1}, \ldots, \vartheta_{i,j-1}^{N+1}, \ldots$ having already been determined. Define a tentative temperature value $\hat{\vartheta}$ as

$$\hat{\vartheta}_{i,j}^{N+1} = a_{i,j}\vartheta_{i+1,j}^{N} + b_{i,j}\vartheta_{i-1,j}^{N+1} + c_{i,j}\vartheta_{i,j+1}^{N} + d_{i,j}\vartheta_{i,j-1}^{N+1} + e_{i,j}F_{i,j} \quad (13)$$

where the most current temperature values are used at those points where they are available. Then, the temperature $\vartheta_{i,j}^{N+1}$ is evaluated as

$$\vartheta_{i,j}^{N+1} = \vartheta_{i,j}^{N} + \omega(\hat{\vartheta}_{i,j}^{N+1} - \vartheta_{i,j}^{N}) \quad (14)$$

where ω is the extrapolation factor. On the basis of preliminary computational experiments, it was found that the most rapid convergence of the iteration scheme was achieved with an ω value of approximately 1·95.

The boundary condition for large ρ, equation (4c), was applied at $\rho = 1500$ in two alternate ways, either as $\vartheta = 0$ or as $\vartheta = 1/\rho$. The ϑ solutions corresponding to these alternate representations of the boundary conditions were essentially identical.

A total of 4619 mesh points were employed in the computations, the distribution of the points being made to accommodate the rapidity of the temperature variations.

Once the temperature field has been determined, various quantities of interest may be evaluated. Of particular relevance to the subsequent treatment of the interaction between the solid and the contiguous cylindrical conductor, Fig. 1(a), is the rate of heat transfer passing through the circular area $0 \leqslant \rho \leqslant 1$ on the surface. To this end, let Q_j^* be defined as

$$Q_j^* = 2\pi \int_0^1 \left(-\frac{\partial\vartheta}{\partial Z}\right)_{Z=0} \rho \, d\rho \quad (15a)$$

$$= 2\pi Bi \int_1^{\bar{\rho}} \vartheta_{Z=0}\rho \, d\rho + 2\pi\bar{\rho}^2 \int_0^{\pi/2} \left(-\frac{\partial\vartheta}{\partial\rho}\right)_{\rho=\bar{\rho}} \sin\varphi \, d\varphi \quad (15b)$$

in which $\bar{\rho}$ is any value of the radial coordinate $\rho > 1$. The derivative $(\partial\vartheta/\partial Z)_{Z=0}$ that would otherwise appear in the first term of equation (15b) has been replaced by $Bi\vartheta$ in accordance with equation (4b).

By making use of equation (2), it is readily demonstrated that the rate of heat transfer Q_j passing through the circular area $0 \leqslant \rho \leqslant 1$ on the surface is given by

$$Q_j = r_0 k(T_j - T_w)Q_j^* + h\pi r_0^2(T_\infty - T_w) \quad (16)$$

where the first term stems from the disturbance temperature field and the second term stems from the temperature field in the absence of the local surface heat sink. Therefore, Q_j^* may be regarded as a dimensionless heat transfer rate associated with the disturbance temperature field.

Numerical values of Q_j^* were evaluated from both equations (15a) and (15b), the indicated integrations being performed by both Simpson's rule and the trapezoidal rule. Inasmuch as equation (15b) avoids the singularity in $(\partial\vartheta/\partial Z)_{Z=0}$ at $\rho = 1$, the Q_j^* obtained from its evaluation are believed to be more accurate than those obtained from the evaluation of equation (15a). The Simpson's rule and trapezoidal integrations yielded essentially identical results. Since the ϑ solutions depend parametrically only on the Biot number Bi, so also do the numerical values of Q_j^*.

Some indication of the accuracy of the present solutions may be made by comparing the Q_j^* value of 4·001 for $Bi = 0$ with the exact result

$Q_j^* = 4$ [2]. The level of agreement is excellent, thereby leading confidence to the accuracy of the present results. Further comparison cannot be made inasmuch as no other numerical information on the problem is available in the literature besides that cited above.

Numerical results for Q_j^*, as well as for other quantities of interest, will be presented in the next section.

HEAT TRANSFER AND TEMPERATURE RESULTS

Solutions for the dimensionless disturbance temperature were carried out for parametric values of the Biot number $Bi(= hr_0/k)$ in the range 0–10. Heat transfer and temperature results based on these solutions will now be presented.

The significance of the quantity Q_j^* has already been discussed. It is a dimensionless heat transfer rate associated with the disturbance temperature field. In particular, due to the disturbance temperature field, the rate of heat transfer passing through the circular area $0 \leqslant (r/r_0) \leqslant 1$ on the surface is $r_0 k(T_j - T_w)Q_j^*$ [see equation (16)]. The dependence of Q_j^* on the Biot number is shown in Fig. 3 for the range $0 \leqslant Bi \leqslant 10$. An inset is also provided to facilitate accurate reading of Q_j^* in the range $0 \leqslant Bi \leqslant 1$, where high reading accuracy would otherwise be difficult to achieve owing to the sharp rise of the curve.

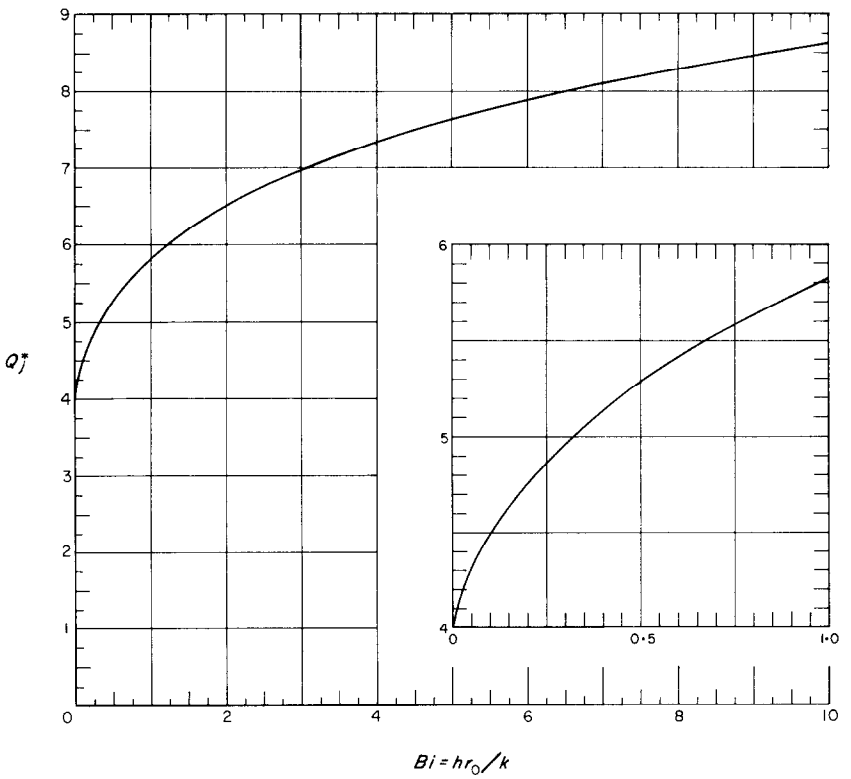

FIG. 3. Dimensionless heat transfer rate associated with the disturbance temperature field.

Inspection of the figure shows that Q_j^* increases monotonically with increasing Bi. This trend is physically reasonable, inasmuch as the convective heat loss in the region $r/r_0 > 1$

increases with increasing Bi, thereby necessitating a corresponding increase in the inflow of heat through the circular region $0 \leqslant r/r_0 \leqslant 1$.

As will be demonstrated later, the results for Q_j^* will play a key role in the evaluation of temperature measurement errors as well as in the calculation of heat transfer rates for pin fins and for cylindrical conductors in general.

The next pair of figures also deals with results which pertain to the surface of solid, but for the region $r/r_0 > 1$ (the region where convective exchange takes place). Let the surface temperature distribution $T(r/r_0, \pi/2) \equiv T_{surf}$ and, consistent with equation (2),† let

$$\vartheta_{surf} = \frac{T_w - T_{surf}}{T_w - T_j}. \tag{17}$$

Since $T_w - T_j$ represents the magnitude of the imposed temperature disturbance, the distribution of ϑ_{surf} with r/r_0 gives the decay of the imposed disturbance along the surface. This information is presented in Fig. 4, where the various curves are parameterized by the Biot number hr_0/k. The continuation of the curves for larger r/r_0 is shown in the inset.

From the figure, it is seen that the decay of the temperature disturbance is relatively rapid in the neighborhood of $r/r_0 = 1$ and becomes more gradual at larger r/r_0. The magnitude of the Biot number has a significant effect on the rapidity of the decay, with the decay being markedly faster at higher values of Biot number. Thus, for example, a 5 per cent residue of the imposed disturbance is achieved at $r/r_0 = 13$ and 1·4, respectively for Biot numbers of 0 and 10.

Whereas ϑ_{surf} compares the local temperature disturbance $T_w - T_{surf}$ with the imposed disturbance $T_w - T_j$, one may be equally interested in comparing the local disturbance with the temperature $T_w - T_\infty$, which is characteristic of the problem. Indeed, it appears reasonable to regard the magnitude of the ratio $(T_w - T_{surf})/(T_w - T_\infty)$ as an indicator of whether or not the disturbance has a locally significant effect on the thermal processes at the surface (e.g. on the local convective heat loss). It is readily verified that

$$\frac{T_w - T_{surf}}{T_w - T_\infty} = \left[\frac{T_w - T_{surf}}{T_w - T_j}\right]\left[\frac{T_w - T_j}{T_w - T_\infty}\right]. \tag{18}$$

The first bracketed quantity on the right is given by Fig. 4, while the second bracket represents a constant, the determination of which will be discussed later. Thus, the distribution curves for $(T_w - T_{surf})/(T_w - T_\infty)$ are identical to those of Fig. 4, except for a multiplicative constant.

On the basis of the foregoing, one may estimate the region of influence of the disturbance. Suppose that the disturbance is judged to have negligible influence when $(T_w - T_{surf})/(T_w - T_\infty) \leqslant 0{\cdot}01$. If $(T_w - T_j)/(T_w - T_\infty) = 0{\cdot}1$,* then the aforementioned condition is met when $r/r_0 = 6$ and 1·2, respectively for Biot numbers of 0 and 10. It may thus be concluded that the region of influence of the disturbance is not very large.

The results of Fig. 4 may also be employed to calculate the local surface heat flux in the region $r/r_0 > 1$. Upon applying Fourier's law to equation (2), there follows

$$\frac{qr_0}{k(T_w - T_\infty)} = Bi\left\{1 - \vartheta_{surf}\left[\frac{T_w - T_j}{T_w - T_\infty}\right]\right\} \tag{19}$$

in which equation (4b) has been used. Within the braces, the first term corresponds to the local surface heat flux in the absence of the disturbance, while the second term is due to the disturbance. The distribution curves of ϑ_{surf} are those of Fig. 4.

Figure 5 has been prepared to illustrate the surface variation of the local heat flux. The figure is subdivided into three sections, respectively for $Bi = 0{\cdot}1$, 1 and 10. In each section, curves of $qr_0/k(T_w - T_\infty)$ are plotted as a function of r/r_0 for parametric values of $(T_w -$

† Note that $\bar{T} = T_w$ when $z = 0$.

* A high value if the disturbance is due to a thermocouple.

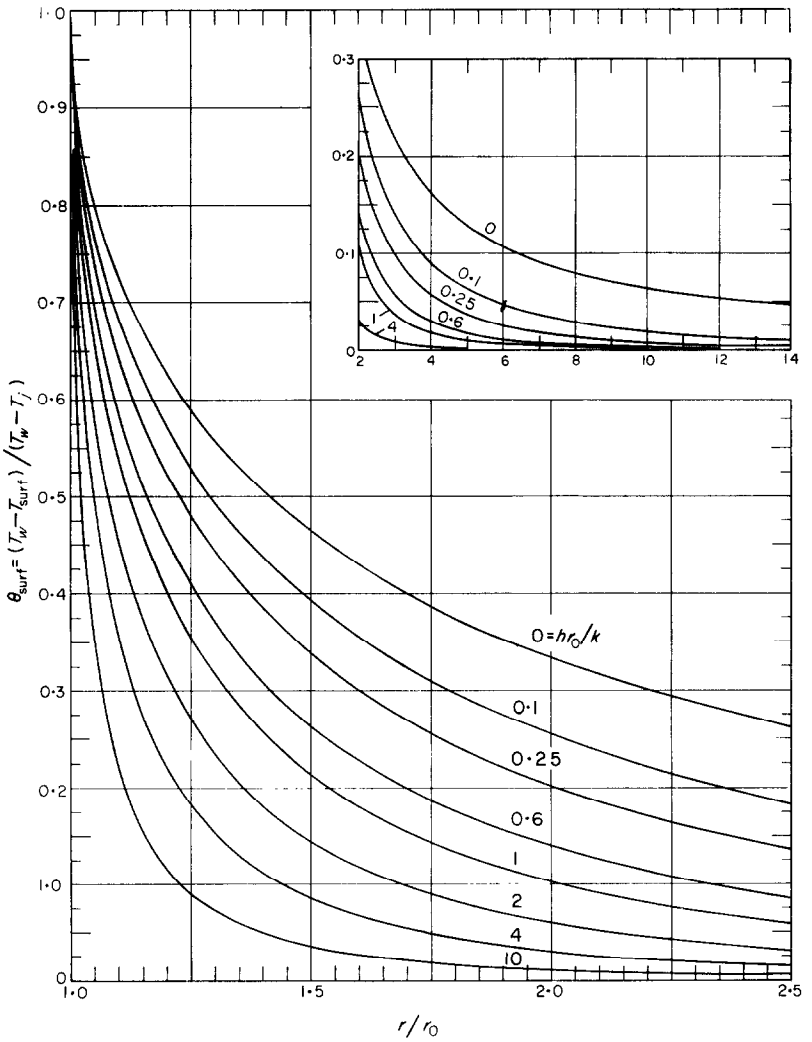

FIG. 4. Surface temperature disturbance ($T_w - T_{surf}$) relative to the imposed disturbance ($T_w - T_j$).

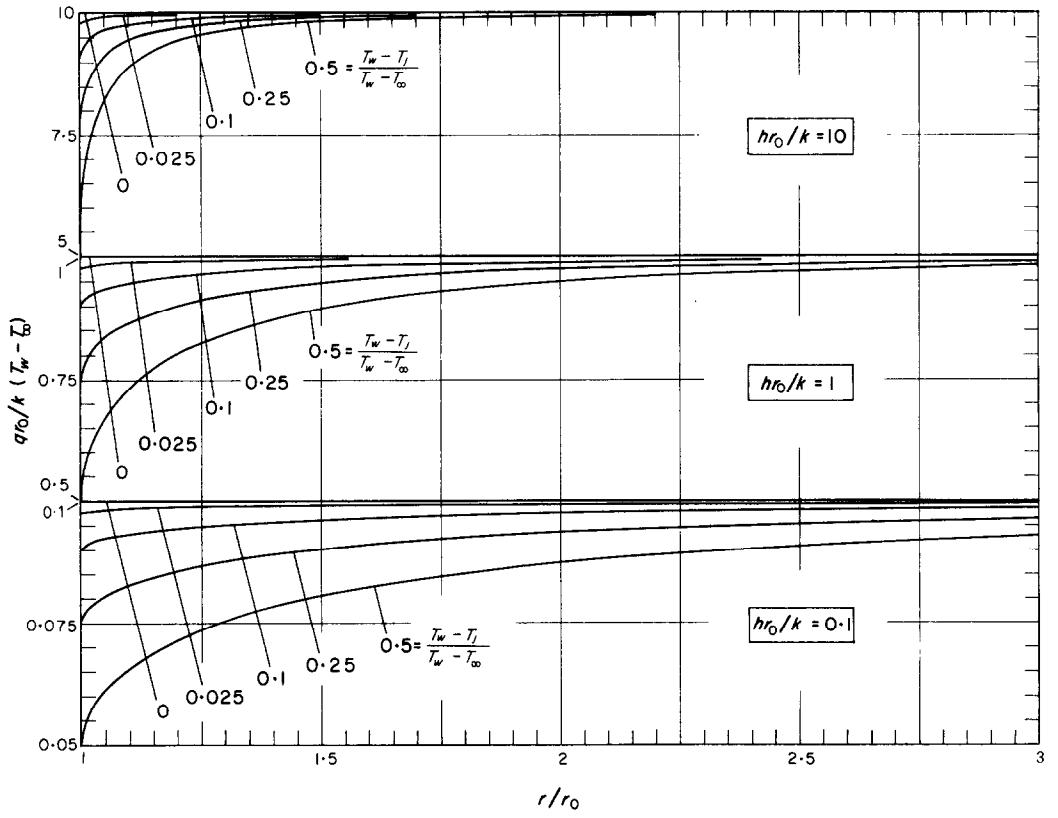

FIG. 5. Local surface heat flux.

$T_j)/(T_w - T_\infty)$ ranging from 0 to 0·5. The results of the figure show that the lower the value of the Biot number, the more sensitive is the local surface heat flux to the presence of the disturbance. In particular, the range of influence of the disturbance increases substantially as the Biot number is reduced.

Attention is now turned to the temperature distribution within the solid. A meaningful dimensionless representation of the temperature distribution, involving the known quantities T_w and T_∞, is embodied in the grouping $(T - T_w)/(T_w - T_\infty)$. From equation (2), one has

$$\frac{T - T_w}{T_w - T_\infty} = BiZ - \vartheta\left[\frac{T_w - T_j}{T_w - T_\infty}\right]. \qquad (20)$$

It is seen that the temperature field consists of two components: a linearly increasing portion corresponding to the absence of the surface heat sink and a disturbance portion due to the surface sink. In the special case of $Bi = 0$, the first component vanishes. Representative temperature distributions are presented herein for two Biot numbers, 0 and 1.

Considering first the case of $Bi = 0$, it is seen that the distribution of $(T - T_w)/(T_w - T_\infty)$ is, except for a multiplicative constant, the same as the distribution of ϑ. Therefore, it suffices to present only the ϑ distribution. A contour diagram, showing lines of constant ϑ, has been constructed and appears in Fig. 6. The curves appearing therein are labeled according to the ϑ values they represent. In physical terms, the abscissa axis is the surface of the solid, while

the ordinate axis is the symmetry line that passes perpendicularly through the center of the circular region $0 \leqslant r \leqslant r_0$ which lies on the surface. This region itself is represented by the segment of the abscissa between 0 and 1. The spherical coordinates r, φ are indicated on the figure, with the angles being marked along the upper and right-hand axes.

$r > r_0$, where the adiabatic boundary condition prevails, the isotherms intersect the surface at right angles.

It is also interesting to compare the findings of Fig. 6 with what would have resulted had the model of [1] been adapted. Following that model, it would have been assumed that the hemispherical region $0 \leqslant r \leqslant r_0$, $0 \leqslant \varphi \leqslant \pi/2$

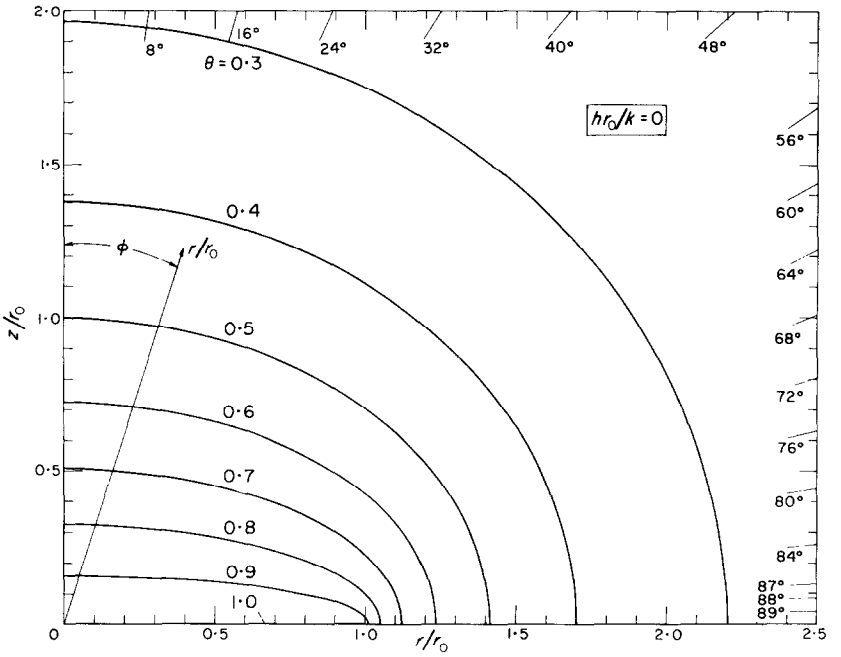

FIG. 6. Isotherms of the disturbance temperature field within the solid, $hr_0/k = 0$.

Inspection of the figure reveals that in the neighborhood of the surface region $r < r_0$, the isotherms are drawn tightly together and are nearly parallel to the trace of the circle. On the other hand, as the radial coordinate increases, the spacing between the isotherms becomes larger and the isotherms themselves tend to become semi-circular in form. Indeed, for positions characterized by sufficiently large r, the region $0 \leqslant r \leqslant r_0$ on the surface appears to be, in effect, a point source (or sink) of heat. It may also be noted that at surface locations is isothermal with $\vartheta = 1$ throughout. This is clearly at variance with the results of Fig. 6. Furthermore, the aforementioned simplified model yields $Q_j^* = 2\pi$, which is substantially in error compared with the result $Q_j^* = 4$.

Consideration may now be given to the temperature distribution results for $Bi = 1$. As indicated in equation (20), the dimensionless temperature field $(T - T_w)/(T_w - T_\infty)$ is synthesized by superposing a linear contribution on the disturbance distribution ϑ, the latter being weighted by $(T_w - T_j)/(T_w - T_\infty)$. It is

revealing to examine both the disturbance and the resultant temperature fields. To this end, Figs. 7(a) and 7(b) have been prepared. The first of these figures is a contour diagram showing the isotherms of the disturbance temperature ϑ. The structure of the figure is identical to that of Fig. 6. There are, however, distinct differences in the results appearing in Figs. 6 and 7(a). In particular, with increasing r, the isotherms of Fig. 7(a) do not tend toward a semi-circular shape as do those of Fig. 6. The reason for this different behavior is that for $Bi > 0$, the surface $r > r_0$ actively participates in the heat transfer process, causing ϑ to drop off rapidly with r at points adjacent to the surface.

The resultant temperature field for $Bi = 1$ is shown in Fig. 7(b), wherein the contribution of the ϑ distribution of Fig. 7(b) is weighted by $(T_w - T_j)/(T_w - T_\infty) = 0{\cdot}25$. The isotherms are labeled according to $(T - T_w)/(T_w - T_\infty)$. In the absence of the surface heat sink, the isotherms

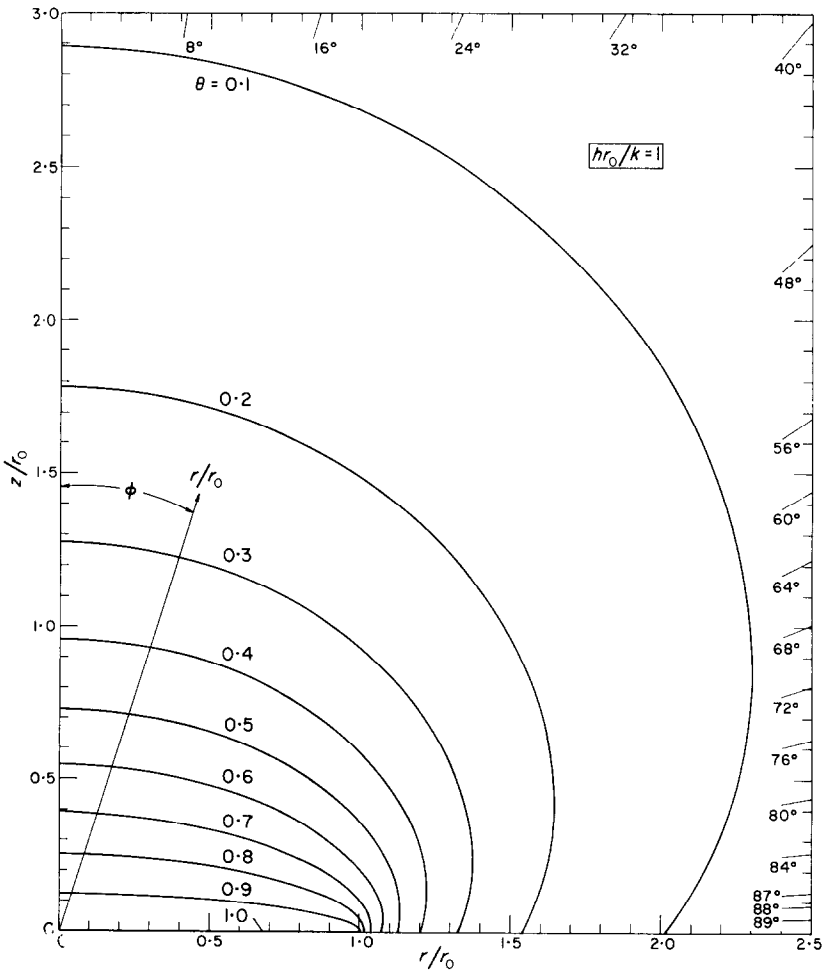

FIG. 7(a). Isotherms of the disturbance temperature field within the solid, $hr_0/k = 1$.

would be horizontal lines whose position is given by $(T - T_w)/(T_w - T_\infty) = z/r_0$. The presence of the sink causes a displacement of the isotherm pattern in the neighborhood of the sink. With increasing distance from the sink, the displacement of the isotherms diminishes rapidly pictured in Fig. 1(a).* Let T_w denote the surface temperature in the absence of the thermocouple, while T_j is the temperature at the junction of the thermocouple and the solid. Correspondingly, $T_w - T_j$ is the measurement error owing to the presence of the thermocouple. The surface

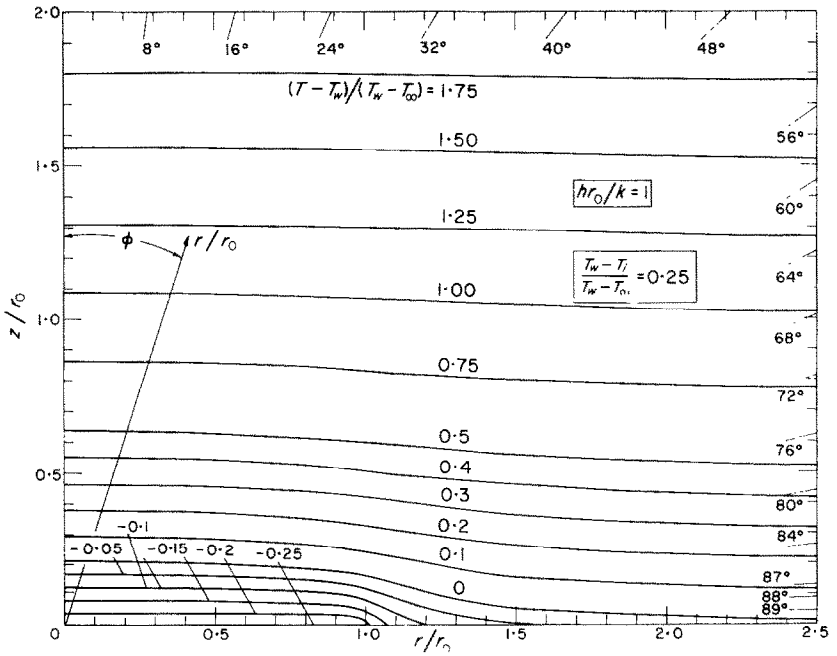

FIG. 7(b). Isotherms of the resultant temperature field within the solid, $hr_0/k = 1$ and $(T_w - T_j)/(T_w - T_\infty) = 0{\cdot}25$.

so that, for example, the 1·75 isotherm is very nearly coincident with the line $z/r_0 = 1{\cdot}75$. A similar rapid damping of the isotherm shift is in evidence as one moves along the surface.

ERRORS IN SURFACE TEMPERATURE MEASUREMENT

Consider now the case in which a thermocouple is affixed to the surface of a solid as of the solid exchanges heat by convection with a fluid environment having temperature T_∞ and heat transfer coefficient h.

* It should be noted that most techniques of affixing the thermocouple to the surface (for instance, with epoxy or solder, or by welding) generally give rise to an irregular geometry in the neighborhood of the thermocouple–surface interface. The detailed study of the complex heat transfer processes in this region is beyond the scope of the present investigation.

The junction temperature T_j is unknown, and its determination is the goal of the forthcoming analysis. As a first step, it is necessary to describe the heat transfer processes in the thermocouple. Suppose that a thermocouple lead is made up of one or two metallic wires plus insulation. Heat is transported axially along the lead by conduction, with most of the heat carried by the wires. The insulation functions primarily as a thermal resistance for lateral heat flow from the surface of the wire (or wires) to the fluid environment. The thermal boundary layer surrounding the lead also plays a similar role, acting in series with the insulation.

Let $\overline{kA}$ represent the conductivity-area product for axial heat conduction in the lead and let R be a thermal resistance such that $(T - T_\infty)/R$ is the rate of lateral heat loss per unit length of the lead. Then, adopting the one-dimensional model of fin theory, the energy balance on a unit length of lead can be written as

$$\overline{kA}\frac{d^2T}{dx^2} - \frac{T - T_\infty}{R} = 0 \qquad (21)$$

where x is the axial coordinate along the lead and $T = T(x)$. If $x = 0$ denotes the junction of the thermocouple and the solid, and $x = L$ is the other extremity of the thermocouple, then the boundary conditions may be stated as

$$T(0) = T_j, \quad (dT/dx)_L = 0. \qquad (21a)$$

The zero derivative condition at $x = L$ is common in fin theory and is highly plausible in the present problem since L is generally much greater than the radius of the wire.

The evaluation of $\overline{kA}$ and R is relatively straightforward when the lead consists of a single insulated or uninsulated metallic wire. When there are two wires, the evaluation of the aforementioned quantities requires some finesse, as is discussed in [9, 10]. In particular, if there are two wires each of radius r_1, it is customary to think in terms of an equivalent single wire whose radius is $r_0 = 2\sqrt{r_1}$.

The solution of equations (21) and (21a) yields $T = T(x)$, and subsequent application of Fourier's law leads to an expression for the rate of heat transfer Q_j passing through the area of contact between the thermocouple and the solid, that is

$$Q_j = (T_\infty - T_j)\sqrt{(\overline{kA}/R)}\tanh\,[L/\sqrt{(\overline{kA}R)}]. \qquad (22)$$

Continuity of heat flux at the junction of the thermocouple and the solid requires that the Q_j expressed by equations (16) and (22) be identical. Upon equating the Q_j and rearranging, one gets

$$\frac{T_w - T_j}{T_w - T_\infty} = \frac{\chi - (hr_0/k)}{\chi + Q_j^*/\pi} \qquad (23)$$

in which

$$\chi = \frac{\sqrt{(\overline{kA}/R)}}{\pi r_0 k}\tanh\,[L/\sqrt{(\overline{kA}R)}]. \qquad (24)$$

The quantity $(T_w - T_j)$ is the error in the temperature measurement owing to the presence of the thermocouple, and $(T_w - T_j)/(T_w - T_\infty)$ is the relative error taken with respect to the characteristic temperature difference $(T_w - T_\infty)$. χ can be regarded as a ratio of conductances, with $\sqrt{(\overline{kA}/R)}$ representing the geometric mean conductance of the thermocouple lead and r_0k representing the conductance of the solid. Q_j^* is given as a function of the Biot number $(= hr_0/k)$ in Fig. 3.

The temperature measurement error is readily evaluated from equations (23) and (24). Figure 8 has been prepared to illustrate the results. The lower portion of the figure spans the χ range from 0 to 16, while the upper part of the figure facilitates accurate reading for the range of small χ. The curves are parameterized by the Biot number, which, for thermocouple applications, is typically between 0 and 0·5.

When $\chi > hr_0/k$ and $T_w > T_\infty$, the measured temperature T_j is below the actual surface temperature T_w. That is, the presence of the thermocouple causes a local depression in the surface temperature. Furthermore, for these

conditions, increases in χ accentuate the measurement error, while increases in hr_0/k tend to reduce the temperature error. If the thermocouple is extremely well insulated so that R is very large, it is possible, at least in principle, that T_j will exceed T_w (when $T_w > T_\infty$). This possibility is, however, unlikely in practice.

cylindrical conductors. In reality, the presence of the fin or conductor alters the temperature field of the solid, so that the base temperature of the fin or conductor is different from T_w. The effect of a thus-altered base temperature on the heat transfer from fins and other cylindrical conductors will now be evaluated.

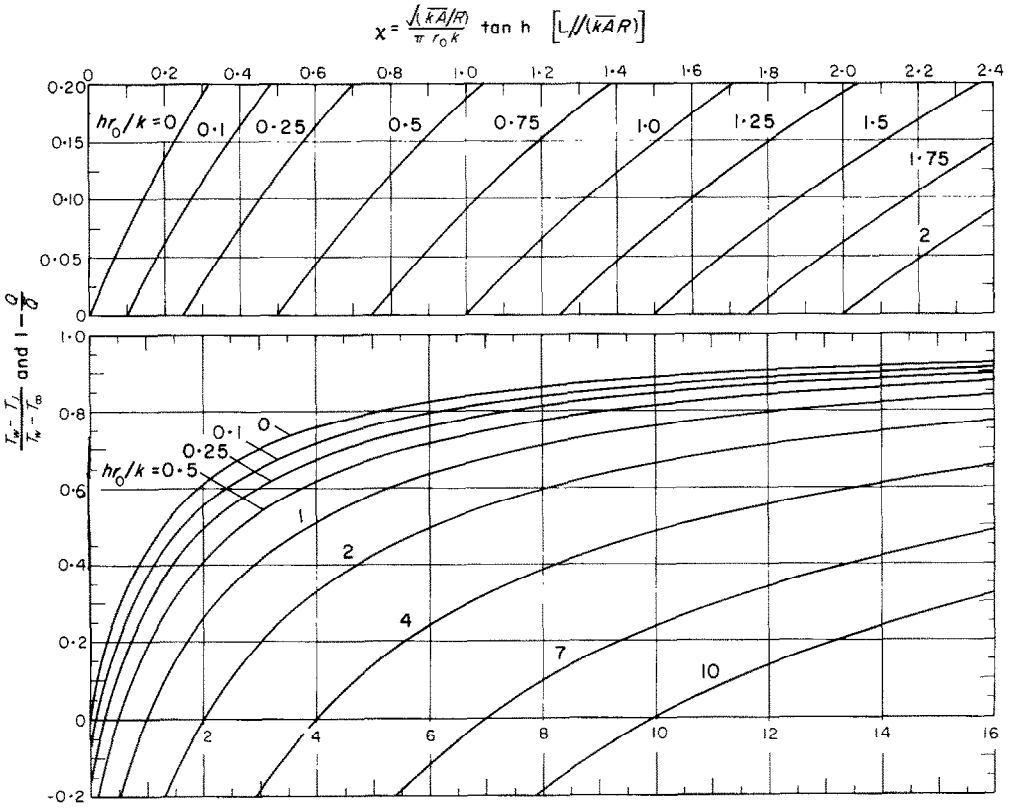

FIG. 8. Temperature measurement error and fin heat transfer ratio.

HEAT TRANSFER FROM FINS AND OTHER CYLINDRICAL CONDUCTORS

In the computation of heat transfer rates for pin fins, it is customary to assume that the fin base temperature is equal to the surface temperature T_w of the solid in the absence of the fin. A similar assumption is made in computing the heat transfer from other surface-mounted

Let Q denote the rate of heat transfer from a pin fin or cylindrical conductor whose base temperature T_j is determined by the interaction between the fin (or conductor) and the solid to which it is affixed. T_j can be evaluated directly from equations (23) and (24), where now, $\overline{kA} = k_f \pi r_0^2$ and $R = (2\pi r_0 h_f)^{-1}$, the subscript f denoting fin (or conductor). Furthermore,

from equation (22), it follows that $Q \sim (T_\infty - T_j)$.

Next, denote by $\tilde{Q}$ the fin heat transfer computed in the conventional manner, that is, assuming that the base temperature is equal to T_w. Thus, $\tilde{Q} \sim (T_\infty - T_w)$ in accordance with equation (22).

The effect of accounting for the true base temperature is manifested in the departure of $Q/\tilde{Q}$ from unity. In light of the foregoing, $Q/\tilde{Q} = (T_j - T_\infty)/(T_w - T_\infty)$, or

$$\frac{Q}{\tilde{Q}} = 1 - \frac{T_w - T_j}{T_w - T_\infty} \tag{25}$$

where the temperature ratio appearing on the right-hand side of equation (25) is expressed by equation (23). A necessary condition for any properly designed fin is that $\chi > hr_0/k$ (otherwise the fin would diminish, rather than augment, the surface heat loss). Correspondingly, $(T_w - T_j)/(T_w - T_\infty) > 0$ and $Q/\tilde{Q} < 1$. That is, the accounting of the base temperature depression due to the presence of the fin gives a lower heat transfer rate than that calculated in the conventional manner.

The $Q/\tilde{Q}$ ratio is readily evaluated from equation (25) in conjunction with equations (23) and (24). In addition, numerical values of $1 - (Q/\tilde{Q})$ are plotted in Fig. 8 for parametric values of χ and hr_0/k. Keeping in mind that $\chi > hr_0/k$ for fins, it is seen that the effect of the base surface depression is accentuated with increasing χ and is diminished with increasing hr_0/k. In other words, the larger the fin heat loss relative to that from the surface itself, the larger are the deviations of $Q/\tilde{Q}$ from unity.

If the surface-mounted conductor has a very low thermal conductivity (i.e. an insulator), the $Q/\tilde{Q}$ may exceed unity.

REFERENCES

1. C. D. HENNING and R. PARKER, Transient response of an intrinsic thermocouple, *J. Heat Transfer* **89C**, 146–154 (1967).
2. H. GRÖBER, S. ERK and U. GRIGULL, *Fundamentals of Heat Transfer*, 3rd. Edn. McGraw-Hill, New York (1961).
3. E. POLLMANN, Temperatures and stresses on hollow blades for gas turbines, *NACA* TM 1183 (1947).
4. L. M. K. BOELTER, F. E. ROMIE, A. G. GUIBERT and M. A. MILLER, An investigation of aircraft heaters. XXVIII—Equations for steady-state temperature distribution caused by thermal sources in flat plates applied to calculation of thermocouple errors, heat-meter corrections, and heat transfer by pin-fin plates, *NACA* TN 1452 (1948).
5. L. M. K. BOELTER and R. W. LOCKHART, An investigation of aircraft heaters. XXXV—Thermocouple conduction error observed in measuring surface temperatures, *NACA* TN 2427 (1951).
6. A. R. THOMAS, B. SCHURIN and J. C. MORRIS, Temperature error associated with imbedded thermocouples, *Rev. Scient. Instrum.* **29**, 1045–1046 (1958).
7. D. R. BURNETT, Transient temperature measurement errors in heated slabs for thermocouples located at the insulated surface, *J. Heat Transfer* **83C**, 505–506 (1961).
8. J. V. BECK, Thermocouple temperature disturbances in low conductivity materials, *J. Heat Transfer* **84C**, 124–132 (1962).
9. H. D. BAKER, E. A. RYDER and N. H. BAKER, *Temperature Measurement in Engineering*, Vol. 1, Chapter 7. John Wiley, New York (1953).
10. E. M. SPARROW, Error estimates in temperature measurement, in *Measurement Techniques in Heat Transfer*, AGARD (to be published).

PUITS DE CHALEUR LOCAL SUR UNE SURFACE REFROIDIE PAR CONVECTION. APPLICATION À L'ERREUR SUR LES MESURES DE TEMPÉRATURE

Résumé—Les processus thermiques associés avec la présence d'un puits (ou d'une source) de chaleur local sur la surface d'un solide refroidie par convection sont analysés. Le puits est dû à la présence d'un thermocouple monté sur une surface, d'une ailette en aiguille ou d'autres conducteurs montés sur une surface. Dans la première partie de l'article, les résultats du transport de chaleur et les distributions de température pour le solide sont déterminés en général, sans référence à des applications spécifiques. Les résultats sont alors appliqués au cas du thermocouple monté sur une surface, et l'erreur sur la température mesurée et due à la présence du thermocouple est évaluée. Ils sont également appliqués aux ailettes en aiguille et à d'autres conducteurs montés sur une surface, et les flux de chaleur sont calculés en tenant compte de la diminution de la température de la bass due à l'interaction entre l'ailette (ou le conducteur) et le solide. On trouve que le calcul classique qui néglige la dimunution de la température de la base surestime les flux de chaleur.

ÖRTLICHE WÄRMESENKE AN EINER KONVEKTIV GEKÜHLTEN OBERFLÄCHE--EINE ANWENDUNG AUF TEMPERATURMESSFEHLER

Zusammenfassung—Die thermischen Vorgänge in Gegenwart einer örtlichen Wärmesenke (oder Quelle) an einer konvektiv gekühlten Oberfläche eines Körpers wurden analysiert. Die Senke wird durch ein oberflächenverbundenes Thermoelement, eine Nadelrippe oder andere oberflächenverbundene Leiter dargestellt. Im ersten Teil der Arbeit wurden Wärmeübergangsergebnisse und Temperaturverteilungen für den Körper allgemein bestimmt, ohne auf spezielle Anwendungen einzugehen. Die Ergebnisse werden dann auf den Fall des oberflächenverbundenen Thermoelements und auf den Temperaturmessfehler angewandt. Die Anwendung wird erweitert auf Nadelrippen und andere oberflächenverbundene Leiter. Wärmeübergangskoeffizienten werden berechnet unter Berücksichtigung der Depression der Basistemperatur auf Grund der Rippenwirkung. Es zeigt sich, dass die übliche Berechnung, unter Vernachlässigung der Temperaturdepression zu grosse Wärmeübergangskoeffizienten ergibt.

ПРИМЕНЕНИЕ ЛОКАЛЬНОГО ТЕПЛОВОГО СТОКА НА ПОВЕРХНОСТИ ПРИ ОХЛАЖДЕНИИ СВОБОДНОЙ КОНВЕКЦИЕЙ ДЛЯ ОПРЕДЕЛЕНИЯ ПОГРЕШНОСТИ ПРИ ИЗМЕРЕНИИ ТЕМПЕРАТУРЫ

Аннотация—Анализируется тепловой процесс при наличии локального стока (или источника) тепла на поверхности твердого тела, охлаждаемой свободной конвекцией. Сток тепла создается расположенной на поверхности игольчатой термопарой или другим проводником. В первой части статьи результаты по теплообмену и распределению температуры представлены в общем виде без ссылок на частное применение. Затем результаты применяются для случая поверхностной термопары. Вычислена погрешность измерения температуры, вызванная наличием термопары. Рассмотрено применение к булавочным ребрам и другим расположенным на поверхности проводникам. Рассчитаны скорости теплообмена с учетом понижения температуры основания, вызванного взаимодействием ребра (или проводника) с твердым телом. Обнаружено, что обычные методы расчета, где не учитывается понижение температуры основания, дают завышение результатов скорости теплообмена.